Hemodynamic Analysis for Olfactory Perceptual Degradation Assessment Using Generalized Type-2 Fuzzy Regression

Mousumi Laha, Amit Konar, Senior Member, IEEE and Pratyusha Rakshit and Atulya K. Nagar

***Abstract*— Olfactory perceptual degradation refers to the inability of people to recognize the variation in concentration levels of olfactory stimuli. The paper attempts to assess the degree of olfactory perceptual degradation of subjects from their hemodynamic response to olfactory stimuli. This is done in 2 phases. In the first (training) phase, a regression model is developed to assess the degree of concentration levels of an olfactory stimulus by a subject from her hemodynamic response to the stimulus. In the second (test) phase, the model is employed to predict the possible concentration level experienced by the subject in [0, 100] scale. The difference between the model-predicted response and the oral response (the center value of the qualitative grades) of the subject about her perceived concentration level is regarded as the quantitative measure of the degree of subject's olfactory degradation. The novelty of the present research lies in the design of a General Type-2 fuzzy regression model, which is capable of handling uncertainty due to the presence of intra- and inter-session variations in the brain responses to olfactory stimuli. The attractive feature of the paper lies in adaptive tuning of secondary membership functions to reduce model prediction error in an evolutionary optimization setting. The effect of such adaptation in secondary measures is utilized to adjust the corresponding primary memberships in order to reduce the uncertainty involved in the regression process. The proposed regression model has good prediction accuracy and high time-efficiency as evident from average percentage success rate (PSR) and run-time complexity analysis respectively. The Friedman test undertaken also confirms the superior performance of the proposed technique with other competitive techniques at 95% confidence level.**

***Index Terms*— Olfactory perceptual degradation, Hemodynamic analysis by Functional near-infrared spectroscopy (f-NIRs), Type-2 fuzzy reasoning and regression.**

I. Introduction

Perception, which usually refers to the process of understanding and interpreting stimuli [1], has diversity in the context of reference of specific sensory modalities [2]. Olfaction is one of the primitive modalities of perception for both the humans and other living creatures [3], [4]. In humans, olfaction plays a vital role in food selection [5], and security-awareness of the workers in mines and chemical industries [6], [7]. Olfactory perceptual degradation is often found as an early symptom of the Alzheimer's disease and olfactory disorders [8], [9]. Degradation in olfactory perceptual-ability of humans often is noticed in both recognizing the odors and also their intensity [10]. As recognizing the odors require prior familiarity of the subject with the odors, in this paper, emphasis is given to determine the subjective ability to detect the concentration levels of the stimuli (aromatic substances) presented to assess their olfactory degradation characteristics.

Degradation in olfactory perceptual-ability can be assessed either by analyzing the subjective judgment (in the form of oral response [11]) about her perception on odor concentration or by measuring the oxygen consumption by the brain during the phase of perceiving the olfactory stimuli. It is noted that the oxygenated blood concentration level in the brain increases with an increase in the concentration level of a given olfactory stimulus [12], [13]. Fortunately, the changes in oxygenated blood concentration in the brain can be accurately measured by non-invasive means using a functional Near Infrared spectroscopy (f-NIRs) device. Additionally, the f-NIRs device has better spatial resolution and low computational overhead than the widely used non-invasive brain signal acquisition devices, such as electroencephalography (EEG) [14], justifying its selection for the present application.

Although there is hardly any work of olfactory perceptual degradation studies, there exist traces of works on olfactory perceptual ability studies for human subjects. For instance, in [15] and [16], the authors make attempts to experimentally determine the threshold parameters of concentration levels, representing the ranges of recognizable olfactory stimuli. A couple of recent studies [17], [18] indicate that patients suffering from the Alzheimer's disease exhibit significant differences in epidemiological, patho-physiological and clinical measures of olfactory features with respect to healthy subjects. These studies raise fundamental question: can early Alzheimer's disease be predicted from certain measures of olfactory dysfunction? Recently, researchers are taking keen interest to examine olfactory recognition ability of pleasant/unpleasant odors using brain signals (EEG) [19], [20]. A couple of studies [21], [22] further envisage that pre-frontal and temporal lobes are respectively responsible for odor recognition and encoding in Long-Term Memory (LTM) [23]. Importance of odor intensities/concentrations is also examined on different living creatures [3], [4] to detect/discriminate natural odorants for their survival.

This paper attempts to assess the degradation in olfactory perception for both healthy and (olfactory) diseased subjects. A (fuzzy) regression model is developed with the acquired hemodynamic response of the subject to selected olfactory stimuli as the input and subject's perception about the relative concentration of the stimulus presented as the output. The regression model developed is utilized later to predict the subject's qualitative degree of perception about the olfactory stimuli samples of selected concentrations, and the same

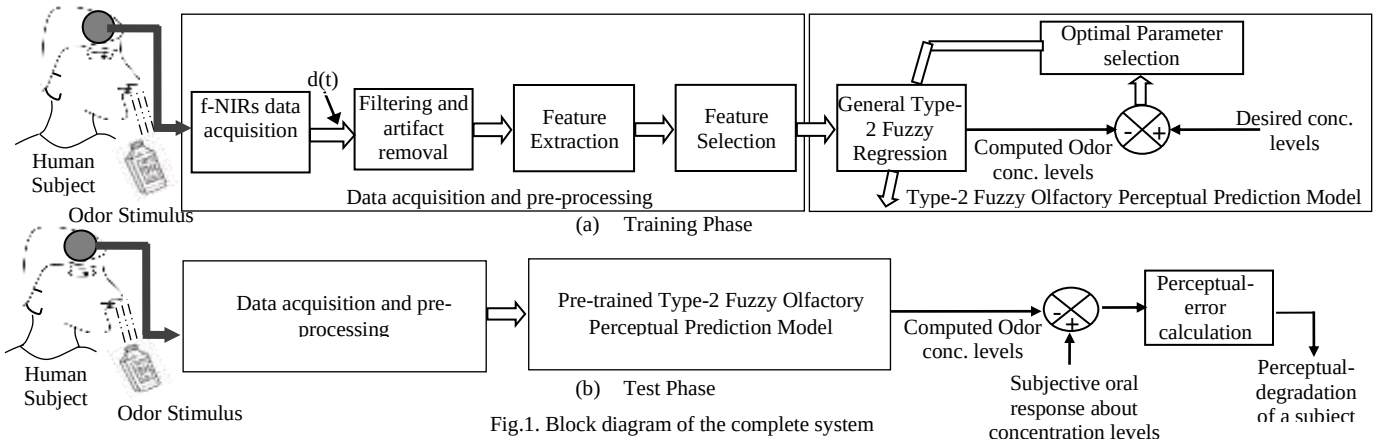

Fig.1. Block diagram of the complete system

stimulus is also presented to the subject again to obtain his/her current qualitative degree of perception about the concentration. The difference between the subject's current degree of perception and the model-predicted degree is used to estimate the measure of his/her perceptual degradation in olfactory processing power of the subject. The idea of assessing degradation in subjective olfactory perception is novel, and useful to check possible olfactory ailments in healthy as well as diseased subjects at early stage of olfactory diseases.

The f-NIRs response obtained from a given source is not free from intra- and inter-session variations because of undesirable parallel thoughts, and artifacts due to eye-blinking and/or non-voluntary motor activations by the subject [24]. Fortunately, the logic of fuzzy sets and in particular type-2 fuzzy counterpart has shown remarkable performance in the past in handling the intra- and inter-session variations [20], [25]. This inspired the present authors to employ type-2 fuzzy sets for the selected application. Relative merits/demerits of type-2 fuzzy sets over classical fuzzy sets are briefly presented below.

A type-1 fuzzy set (FS) represents the degree of precision of a linguistic variable based on the judgment of a single expert in the membership scale of the [0, 1]. So, membership assignment in type-1 FS is crisp [26]. A General Type-2 Fuzzy Set (GT2FS) [27], on the other hand, is a 3-tuple, containing i) a linguistic variable, ii) primary membership of the variable, and iii) a secondary membership grade, representing the degree of precision (certainty) of the primary membership assignment for a given value of the linguistic variable [62]. Here, both the primary and secondary memberships lie in the scale [0, 1]. An Interval Type-2 Fuzzy Set (IT2FS) can be regarded as a special form of GT2FS with secondary membership equal to one for all feasible values of the primary memberships > 0 [28], [29]. The space of primary memberships with secondary grade of membership > 0 is called the *footprint of uncertainty* (FOU) [30]. The FOU is segregated from the rest in the plane of linguistic variable and primary membership by two boundaries, called the Upper and the Lower Membership functions (UMF and LMF), where the UMF ≥ the LMF for all values of the linguistic variable.

Although both IT2FS and GT2FS include subjective opinion of several experts in primary membership assignment, the former lacks the power of representing precision in the degree of primary memberships due to uniformity in secondary memberships over the FOU. Undoubtedly, GT2FS offers better performance in reasoning in presence of intra- and inter-session uncertainty (variations in measurements) in comparison to classical fuzzy and IT2FS, however, at the cost of additional computational overhead. The motivation of the present work is to undertake GT2FS regression with limited computational overhead.

Novelty of the present work lies in the design of a new GT2FS-reasoning based regression model with an aim to reduce uncertainty in the reasoning space by adoption of the following steps. First, a new intuitively selected mapping function is employed to refine the primary memberships based on the measure of both the secondary grade and the primary membership at a given value of the linguistic variable. The proposed mapping function enhances the primary memberships with high secondary grades (i.e., central region of FOU with low uncertainty), but reduces primary memberships lying on the neighborhood bounds of the existing LMF and UMF (i.e., regions of high uncertainty). Consequently, the re-constructed LMF is leveled up, and the reconstructed UMF, produced from the central span of the original FOU, is reduced. Second, the Greatest Lower Bound (GLB) of the refined LMFs and the least upper bound (LUB) of the refined UMFs at the given measurement points are evaluated to compute the upper and lower firing strengths (UFS and LFS) of the fired rules. The introduction of the GLB and the LUB ensures a further reduction in the span of uncertainty of the type-2 fuzzy inference.

Additionally, a corrective feedback to the Gaussian type secondary membership functions of the antecedent variables is given to adjust its variance parameter based on the model produced error with respect to subject's perception about concentration of the stimulus. Besides the above, the fuzzy regression model parameters are optimized using a grid search algorithm [31].

The paper is divided into six sections. In Section II, a schematic overview of the proposed principles of olfactory perceptual-degradation assessment is introduced. Section III is concerned with GT2FS based type-2 fuzzy regression model for perceptual-degradation assessment. Experimental details are covered in Section IV. Performance analysis is

undertaken in Section V. Conclusions are listed in Section VI.

II. Principles and Methodology

The paper introduces a novel technique for the assessment of olfactory perceptual-degradation of the subjects. This is done in 2 phases. In the first (training) phase, a new computational model of type-2 fuzzy regression (reasoning followed by de-fuzzification) is developed to fit the brain (hemodynamic) response of the subject to an aromatic stimulus as the input, and the oral response of the subject about the qualitative degree of concentration perceived by him/her in the form: Very Low, Low, Medium, High and Very High as the output. For convenience of realization, each qualitative grade is defined as sub-intervals of [0, 100], such as [1, 20) for Very Low, [20, 40) for Low, [40, 60) for Medium, [60, 80) for High, and [80, 100] for Very High. Intervals of width 20, instead of absolute value in [0, 100] is utilized to express subject's perceptual response to avoid extensive subject's training for each degree of concentration in [0, 100].

In the test phase, the model response and the subject's (actual) oral response to a known stimulus of selected concentration are extracted, and the difference between these is used as the measure of olfactory degradation of the subject during the period between the training and test phase. For computation of the measure of olfactory degradation, both the subject's oral response and model response should have a uniform representation. Here, the model response being a real scalar, and subject's response being an interval, the subject's response needs to be transformed to a scalar. This is adopted here by taking the centre value of the interval selected by the subject. Fig. 1(a) and (b) respectively represent the schematic overview of the training and test phases.

A. Normalization of the Stimuli

Normalization of the concentration is needed to express the absolute concentration (in mg/L) of the aromatic substance in a fixed interval of [0, 100]. This is done by employing a mapping function $f: x \to y,$ where x and y denote the actual and normalized concentration. Let $x_{\min}$ and $x_{\max}$ be the minimum and maximum values of the measured concentration of the aroma in mg/L. Then for a given concentration $x,$ we define

$$y = Q\left(\frac{100}{x_{\max} - x_{\min}} \times (x - x_{\min})\right). \quad (1)$$

where Q(.) denotes quantized upper ceiling value of the argument.

B. Time-Windowing for Stimulus Presentation and Data Acquisition

The f-NIRs data acquisition in the present set-up is carried out over distinct time-windows across trials. A trial includes presentation of a stimulus of a fixed concentration for 3S, acquisition of f-NIRs data in response to the stimulus over 9S, and acquisition of oral response (OR) of the subject about the possible qualitative degree of concentration level of the stimulus in the next 3S. A trial thus has duration of 15S (Fig.2). A session includes 5 trials for each stimulus of fixed concentration with a rest interval of 3 seconds between two successive trials, thus requiring (15 × 5)S for 5 trials and (3 × 4)S for 4 rest periods with a total duration of 87S (Fig. 2). 5 sessions, each of which represents f-NIRs data collection with distinct concentration of a selected stimulus, are accommodated in a day (Fig.2). To capture the diurnal variations in the f-NIRs response, the data collection process of 5 sessions is repeated over 10 consecutive days (Fig. 3). The above process of stimuli presentation and f-NIRs data and oral response collection is repeated for 10 different olfactory stimuli (Fig.3). Thus for each olfactory stimulus, a set of 10 days × 5 sessions/day × 5 trials/session = 250 trials are employed for each subject. The choice of 9S time interval, preceded by 3S stimulus presentation ensures sufficient elicitation of the neurons to obtain measurable response with appreciable resolution [32].

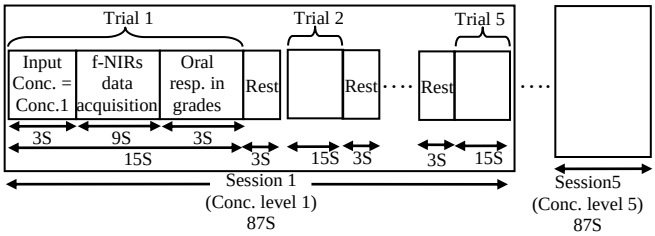

Fig. 2 Schematic representation of a stimulus presentation over a single day

C. Normalization of Acquired Raw f-NIRs data

To normalize the acquired f-NIRs data, the following principle is adopted. Let $C_{HbO_\phi}(t)$ and $C_{HbR_\phi}(t)$ be the oxygenated and de-oxygenated blood response at the ϕ-th channel of the pre-frontal lobe to an olfactory stimulus at time point *t*. It is known that $C_{HbR_\phi}(t) < C_{HbO_\phi}(t)$ for all *t*, from a selected brain region [33], [34]. Thus to normalize $C_{HbO_\phi}(t)$ and $C_{HbR_\phi}(t)$ for a given channel, the following 2 parameters are first evaluated:

$$C_{HbO-Max} = Max_t(C_{HbO_\phi}(t) : t_0 \le t \le t_0 + T, \forall \phi) \quad (2)$$

$$C_{HbR-Min} = Min_t(C_{HbR_\phi}(t) : t_0 \le t \le t_0 + T, \forall \phi) \quad (3)$$

where t_0 and $t_0 + T$ respectively denote the beginning and the end time of an experimental trial for a given stimulus on a selected subject. It is apparent from Fig. 2 that T = 9 seconds. The normalized value of the difference signal

$$d_\phi(t) = C_{HbO_\phi}(t) - C_{HbR_\phi}(t), \quad (4)$$

is obtained as

$$\hat{d}_\phi(t) = \frac{(C_{HbO_\phi}(t) - C_{HbR_\phi}(t))}{C_{HbO-Max} - C_{HbR-Min}}. \quad (5)$$

in the interval [0, 1]. The sampling rate of the f-NIRs device is 7.892 samples/sec.

D. Pre-processing and Filtering of Normalized f-NIRs data

Like EEG, f-NIRs response too suffers from various forms of artifacts. Three most common forms of artifacts that need special mention include: 1) step artifacts, 2) spike artifacts and 3) physiological artifacts [35]. The step artifacts come into play, when there is a change in the surrounding environment. The step artifact can be removed by minimizing

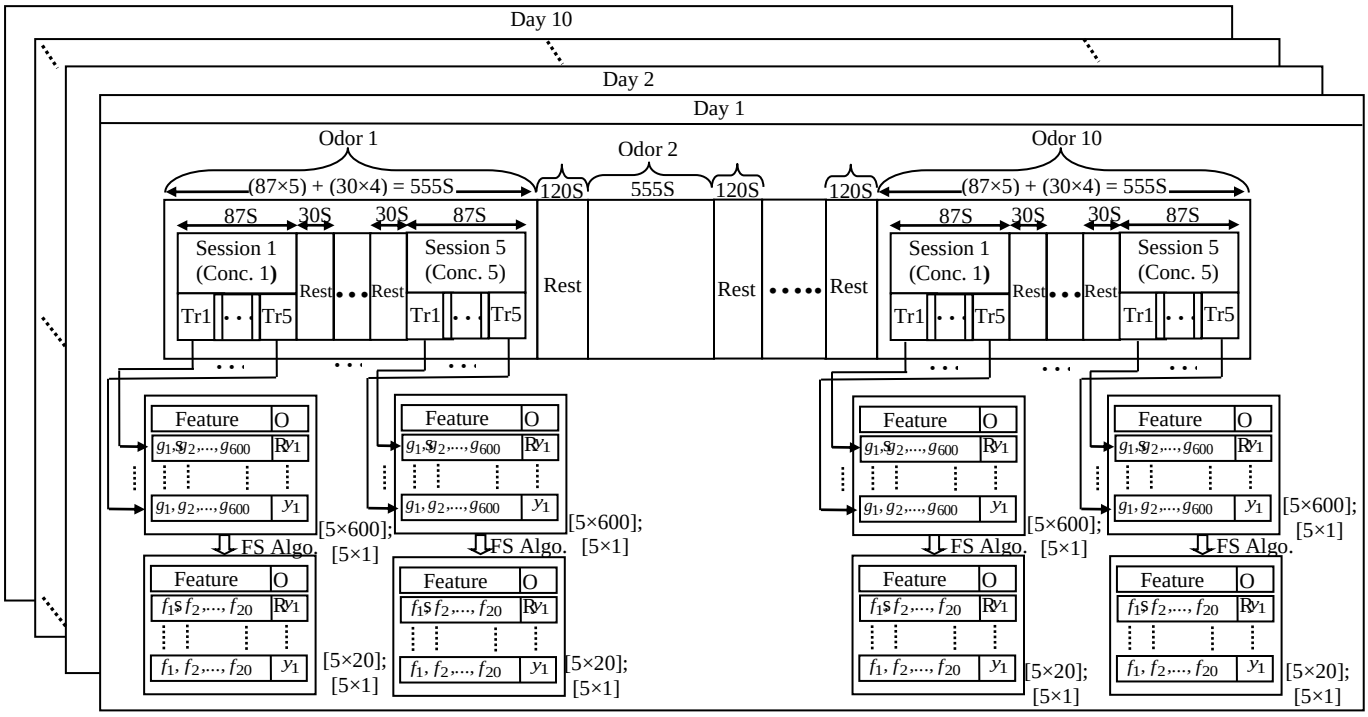

Fig. 3 Stimuli presentation over 5 sessions, each containing 5 trials with same concentration of an aromatic substance, repeated over 10 odors in a day, for feature extraction and feature selection with the whole process repeated over 10 days following a fixed sequence of odor presentation

the variation of the external light and instrumental noise. The spike/motion artifacts are related to decoupling between the electrodes and their assigned positions due to head or muscle movement. They result in abrupt changes in the amplitude of the received signals. For example, a sudden change in the ambient light intensity results in a spike-like noise. Another important artifact is physiological artifact, which may cause different types of physiological noise due to eye-blinking, respiration, heart-beat, blood pressure fluctuations and Mayer wave etc. [35]. To keep the f-NIRs response free from artifacts, the normalized difference signal $\hat{d}_{\phi}(t)$ for $\phi = 1$ to Q channels is passed through a Chebyshev type band pass filter [36] of order 4 with a pass-band of [0.1, 5] Hz. The choice of the Chebyshev band pass filter is induced by its sharp roll-off around the cut-off frequency [37]. Next, the Independent Component Analysis (ICA) [38] has been performed to restore the 20 independent components of the hemodynamic response for 20 channels of the f-NIRs device.

E. Feature Extraction from Filtered f-NIRs data

The artifact-free independent components are processed to extract the important features. The 9 second duration of the f-NIRS data acquisition for each trial, shown in Fig.2, is divided into three equal time-windows of 3 second each (Fig. 4). Here, from each time-window, two distinct types of features, called static and dynamic features, are extracted. Over each 3 seconds time-window, 6 static features, including mean (*M*), variance (σ), signal slope (*sp*), skewness (*sk*), Kurtosis (*ku*) and average energy (*E*) are extracted at fixed time sample points $t = z\tau$ for integer $z = 0, 1, 2, ..., (Z-1)$, where τ is the sampling interval = 1/7.892 seconds $\approx$ 125 milliseconds and *Z* = 3seconds /125 milliseconds = 24 samples. The dynamic features, on the other hand, are obtained by taking the difference of the same static feature over successive time-windows [39]. The computation of the dynamic features is explained briefly below.

Let $\hat{d}_{i,\phi}(t)$ be the filtered *i*-th feature of the ϕ-th channel for i =1 to N_f and ϕ=1 to *Q*. Then the discrete features $\hat{d}_{i,\phi}(t)$ is expressed as $\hat{d}_{i,\phi}(z\tau)$, for $z = 0, 1, 2, ..., (Z-1)$. Now, for the static feature $\hat{d}_{i,\phi}(z\tau)$, the dynamic feature *i* from the ϕ-th channel is obtained by

$$\Delta\hat{d}_{i,\phi}(z\tau) = \hat{d}_{i,\phi}(z\tau) - \hat{d}_{i,\phi}((z-1)\tau) \quad (6)$$

for i =1 to N_f and ϕ=1 to *Q*, $z = 1, 2, ..., (Z-1)$.

In the present application, we have 6 × 3=18 static features and 6 × 2=12 dynamic features (Fig. 4), taken over 3 time-windows in a trial for a given channel. Consequently, we have 18+12 = 30 features for each channel, thereby providing 20 channels × 30 features/channel = total 600 features in a trial for an individual subject. The 600 dimensional feature vector obtained for each trial is denoted by $(g_1, g_2, ..., g_{600})$, where the first 30 features: g_1 through g_{30} correspond to those obtained for channel 1, the next 30 for channel 2, and so on up to channel 20, in a fixed ordered sequence of features for each channel. It is important to mention here that *Q* =20 channels are taken to measure the diversity in f-NIRs response (and so features) across different brain regions. It is noted that with increase in odor concentration, the brain regions corresponding to maximum activation shifts from Orbito-frontal cortex to the Middle frontal region through the Dorso-lateral and Ventro-lateral pre-frontal cortex. The mean and average energy features taken from the channels

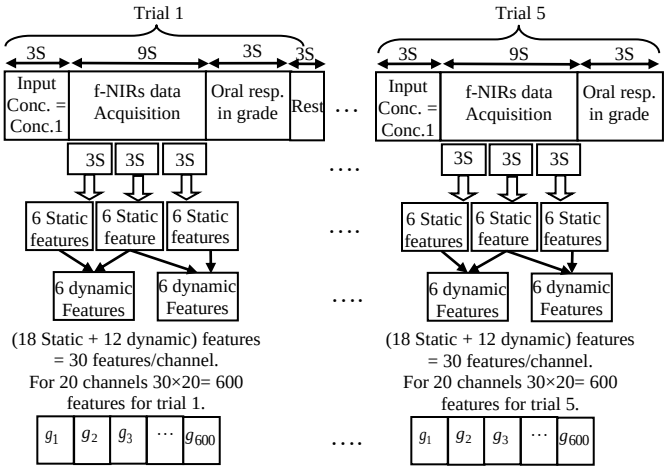

Fig. 4 Static and dynamic feature extraction from the f-NIRs data over each trial

corresponding to maximum brain activation, would increase, while variance, signal slope, skewness and kurtosis features depend largely on the temporal variation of the f-NIRs response, acquired from individual channels. A feature selection algorithm is employed next to uniquely select fewer features from 250 trials, each of 600 dimensional features. A small dimensional feature is preferred as it requires fewer computations and thus is convenient for real-time applications. A reduced feature dimension of 20 serves the purpose as the results, as by increasing feature dimension above 20 does not offer any significant changes in the output of the reasoning algorithm undertaken after feature selection.

F. Feature Selection

There exist a vast literature on feature selection algorithms, including Principal Component Analysis (PCA) [40], Sequential Forward Search (SFS), Sequential Backward Search (SBS), and the like. The PCA algorithm suffers from the fundamental characteristic of selecting linearly independent features. The SFS and the SBS algorithms also suffer from one fundamental problem, well-known as Nesting Effect [41], [42]. Evolutionary feature selection algorithms have shown promising performance in selecting non-linearly independent features as well. This inspired the authors to employ evolutionary algorithm for the present feature selection problem. Differential Evolution (DE) [43] algorithm is one of the widely used evolutionary algorithms that have shown outstanding performance in multimodal single and multi-objective optimization problems. DE is selected from its companion swarm/evolutionary algorithms for its simplicity in coding, small code length and fewer control parameters, and above all the authors' familiarity [44] with the algorithm.

It is already mentioned that during the experiments, same concentration level of a given stimulus is maintained within a session, while different concentration levels of the selected stimulus are presented across distinct sessions. The motivation of the feature selection technique is to identify the minimum set of features, such that the selected features should support minimum intra-session variation and maximum inter-session variations.

To develop this framework of optimization, we need to define certain parameters. Let ${}^{d,s,h}g_i$ be the i-th feature at the h-th trial lying in session s of day d. Similarly, let ${}^{d,s',h'}g_i$ denote the i-th feature at the h'-th trial falling in a different session s' on the same day d. Let ${}^{d,s,h}g_i$ and ${}^{d,s,h'}g_i$ be two features lying in the s-th session. Let J_1 be a measure of intra-session separation, and J_2 be a measure of inter-session separation.

$$J_1 = \sum_{\forall d\in D}\sum_{\forall s}\sum_{\substack{\forall h,h'\in s\\ h\neq h'}}\sum_{\forall i}\left\| {}^{d,s,h}g_i - {}^{d,s,h'}g_i \right\| \tag{7}$$

$$J_2 = \sum_{\forall d\in D}\sum_{\substack{\forall s,\forall s'\\ s\neq s'}}\sum_{\substack{\forall h\in s\\ \forall h'\in s'}}\sum_{\forall i}\left\| {}^{d,s,h}g_i - {}^{d,s',h'}g_i \right\| \tag{8}$$

An attempt is endeavored to maximize J_2 to maintain large inter-session separation, and minimize J_1 to reduce intra-session separation. Let J' be the composite objective function aiming at maximizing J_2 and minimizing J_1 jointly,

$$J' = \frac{J_1}{\eta + J_2}, \tag{9}$$

where, η is a small positive constant. A positive value of η in [0.01, 10] is chosen to optimize J' using a Grid-search optimization algorithm (See Section III). In the present application, the widely used version DE/rand/1/bin has been employed with scale-factor F = 0.7 and crossover with crossover rate C_r = 0.8 have been required to reduce the huge set of features (N = 600) to 20 best features (n). Here, N_f and n respectively denote the total number of features, and the reduced number of features, i.e., $n \le N_f$. Finally, the resulting 20 best features out of 600, hereafter denoted by $f_1, f_2, ..., f_{20}$ are fed to the training instance generation.

G. Training instances generation

The best 20 features, ${}^{d,s,h}f_1$ through ${}^{d,s,h}f_n$ along with the oral response ${}^{d,s,h}y$ for each trial together forms the training instances. Here, for each subject, for each odor the training instances include 10 days × 5 sessions/day × 5 trials/session = 250 trials, each of 20 columns representing input instances and one oral response ${}^{d,s,h}y$, representing the output instance. A database for 10 odors/ subject is prepared for 22 healthy people and 8 brain-diseased people with 250 trials/ odor/ subject.

H. Type-2 Fuzzy Regression for Perceptual-degradation

Lastly, olfactory perceptual degradation in subjects is assessed using a new general type-2 fuzzy regression approach, the details of which are given in Section III.

III. GT2FS-Based Prediction for the Assessment of Olfactory Perceptual-Degradation

This section provides detailed design of GT2FS based prediction for the assessment of subjective perceptual-degradation during the training and the test phases using Mamdami-like approach. The Mamdani-like formulation is required to utilize the consequent GT2FS MFs, which could not be used in case of Takagi-Sugeno-Kang (TSK) GT2FS model [45]. The Mamdani type GT2FS regression yields

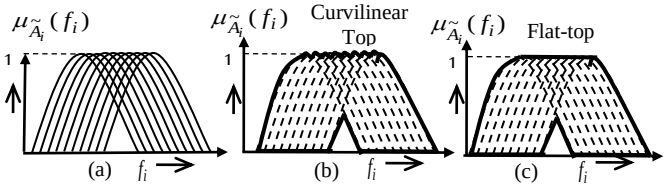

Fig.5. Construction of IT2FS (a) Type-1 MFs for ten days, (b) Computing union of Type-1 MFs, (c) Flat top approximation of Fig. (b)

better performance than its TSK counterpart (Appendix A.1) [65] with respect to percentage success rate (PSR) defined in Section V.

A. Preliminaries on GT2FS

Definition 1: Let X be the universe of discourse of a linguistic variable x. A classical/type-1 fuzzy set A [46], defined on the universe X, is a two-tuple, given by

$$A = \{(x, \mu_A(x)) | \forall x \in X\} \tag{10}$$

where, $\mu_A(x)$, called membership of x in A, is a crisp number in [0, 1] for any $x \in X$. The fuzzy set A is also expressed as

$$A = \int_{x \in X} \mu_A(x) | x \tag{11}$$

where $\int$ represents the union of all feasible $x \in X$.

Definition 2: A General Type-2 Fuzzy Set (GT2FS) [27] $\tilde{A}$ is a 2-tuple, given by

$$\tilde{A} = \{(x,u), \mu_{\tilde{A}(x)}(u)\} \tag{12}$$

where $x \in X$ is a linguistic variable and $\forall u \in J_x \subset [0,1]$ is the primary membership and $\mu_{\tilde{A}(x)}(u)$ is the secondary membership lying in [0, 1].

Definition 3: For a given $x = x'$ the two-dimensional plane comprising u, and $\mu_{\tilde{A}(x')}(u)$ is referred to as a vertical slice $\mu_{\tilde{A}(x)}(u)$. [29].

Definition 4: For a given universe of discourse X of a linguistic variable x, if $\mu_{\tilde{A}(x)}(u) = 1, \forall x \in X$ and $\forall u \in J_x \subseteq [0,1]$, then the type-2 fuzzy set $\tilde{A}$ is called an Interval Type-2 Fuzzy Set (IT2FS) [28].

Definition 5: The Footprint of Uncertainty (FOU) [30] of an IT2FS $\tilde{A}$ represents the union of all feasible type-1 MFs, called embedded fuzzy $A_e(x)$. Formally,

$$FOU(\tilde{A}) = \bigcup_{\forall x \in X} J_x \tag{13}$$

where $J_x = \{(x,u) | u \in [0,1], \mu_{\tilde{A}(x)}(u) > 0\}$.

The FOU indicates the space of uncertainty of the primary membership for all $x \in X$.

Definition 6: The embedded fuzzy set $A_e(x)$ is an arbitrary selected type-1 MF lying in the FOU, i.e., $A_e(x) \in J_x, \forall x \in X$, corresponding to the upper bound of $FOU(\tilde{A})$ is referred to as upper membership function (UMF). This is symbolized as $\overline{FOU(\tilde{A})}$ or $\overline{\mu}_{\tilde{A}}(x), \forall x \in X$ [47]. Analogously, the embedded fuzzy sets that stands for the lower bound of $FOU(\tilde{A})$ are

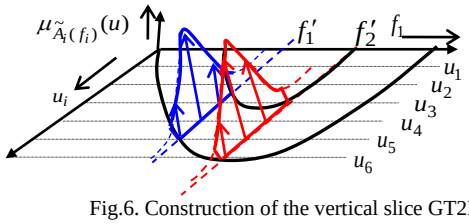

Fig.6. Construction of the vertical slice GT2FS

referred to as lower membership function (LMF). The LMF is generally denoted by $\underline{FOU(\tilde{A})}$ or $\underline{\mu}_{\tilde{A}}(x), \forall x \in X$.

Mathematically,

$$LMF(\tilde{A}) = \underline{\mu}_{\tilde{A}}(x) = \underline{FOU(\tilde{A})} = \min_{\forall x}(A_e(x)) \tag{14}$$

and $$UMF(\tilde{A}) = \overline{\mu}_{\tilde{A}}(x) = \overline{FOU(\tilde{A})} = \max_{\forall x}(A_e(x)). \tag{15}$$

B. Construction of General Type-2 Fuzzy Engine for Regression

A General type-2 fuzzy regression engine is developed here to produce a fuzzy inference about the concentration level of a selected aromatic stimulus experienced by a subject from the selected hemodynamic features.

GT2FS Construction: Let, ${}^{d,s,h}f_i$ be i-th feature extracted on day d of a selected concentration (Conc.) in trial h of session s. The mean and the variance of the feature i over a session s in day d of that concentration are respectively given by

$${}^{d,s}\bar{f}_i = (\sum_{h=1}^{5} {}^{d,s,h}f_i)/5 \tag{16}$$

$${}^{d,s}\sigma_i^2 = \sum_{h=1}^{5} ({}^{d,s,h}f_i - {}^{d,s}\bar{f}_i)^2 / 5. \tag{17}$$

One type-1Gaussian MF $G({}^{d,s}\bar{f}_i, {}^{d,s}\sigma_i^2)$ is prepared to model the variation of the i-th feature extracted on day d in session s. Now, suppose the same experiments is repeated over d = 1 to 10 days. Thus for d =1 to 10, we have 10 such Gaussian MFs $G({}^{d,s}\bar{f}_i, {}^{d,s}\sigma_i^2)$ which are used to develop an IT2FS by the following procedure.

1. The primary membership space of GT2FS $\tilde{A}_i$, for feature f_i, is modeled by taking the union of $G({}^{d,s}\bar{f}_i, {}^{d,s}\sigma_i^2)$, over d=1 to 10 days.

$$\tilde{A}_i(f_i) = \bigcup_{d=1}^{10} G({}^{d,s}\bar{f}_i, {}^{d,s}\sigma_i^2). \tag{18}$$

2. In order to maintain the convexity criteria [47] of the proposed GT2FS, the peaks of the constituent type-1 MFs are joined by a straight line of zero slopes, resulting in a flat-top approximation (Fig. 5(a-c)).

3. Now, at the measurement point $f_i = f_i'$, a Gaussian type secondary membership is constructed with peak at the centre of the FOU. This effectively returns a GT2FS (Fig.6).

It is important to note that, the GT2FS regression engine presented in Fig. 7 is developed for a fixed concentration. Thus for 5 different concentrations, we have 5 distinct fuzzy regression engines. Now, for different concentration we would use different planes of Fig. 8.

To encode the subjective judgment of the perceived odor concentration into type-2 fuzzy sets, the following principle is adopted.

1. If all the choices for 5 trials by the subject are distinctive and disjoint, 5 Gaussian type-1 MFS are constructed with the centre value of the 5 intervals as the mean and 1/10-th of the mean as the variance of the selected Gaussian MFs, where the factor 1/10 is selected heuristically.
2. If out of 5 choices in a session, *v* (< 5) choices belong to a particular grade, then *v* equi-spaced values in the selected interval are used as the means and 1/10-th of the respective means as the variance of the Gaussian MF.
3. If only one choice in a session of 5 possible choices belong to a given grade, then a Gaussian MF is constructed with mean as the centre of the selected interval and a variance = 1/10 the of the mean is adopted.

As sessions involving stimulation with same concentration are invoked repeatedly over fixed number of *d* days, the experimental instances obtained thereof are utilized to construct type-1 Gaussian MF. Finally, a union of the constructed type-1 Gaussian MFs taken over all the *d* days of a selected session (dealing with fixed concentration of the stimulus) is evaluated to yield an interval type-2 fuzzy set for that session.

Type-2 Fuzzy Rules: now we consider one typical rule R_j given by

$$If\ \ f_1\ is\ \tilde{A}_1,\ f_2\ is\ \tilde{A}_2, ...,\ f_n\ is\ \tilde{A}_n, Then\ y\ is\ \tilde{B}_j.$$

Here, $f_i\ is\ \tilde{A}_i$, for feature *i* =1 to *n* of *c*-th concentration denotes the GT2 fuzzy antecedent propositions, the GT2 MF of which is given by $< f_i, u_{\tilde{A}_i}(f_i), \mu(f_i, u_{\tilde{A}_i}(f_i)) >$ where f_i is the linguistic variable, $u_{\tilde{A}_i}(f_i)$ is the primary membership function (MF) and $\mu(f_i, u_{\tilde{A}_i}(f_i))$ is the secondary membership at a given f_i for *m* discretizations $u_{i,1}, u_{i,2}, ..., u_{i,m}$ along the u_i-axis. The choice of *m* is an important issue to determine system performance, optimized later by grid-search algorithm. Theoretically, larger the value of *m*, the smaller is the objective function (*J*). However, it is noted that for $m > 6$, there is no further improvement in *J* and so $m = 6$ is chosen as the system parameter. Similarly, $y\ is\ \tilde{B}_j$ is a vertical slice based GT2FS consequent proposition, whose GT2 MF is given by $< y_i, u_{\tilde{B}_j}(y_j), \mu(y_j, u_{\tilde{B}_j}(y_j)) >$.

Construction of Secondary Membership function: To construct the secondary membership $\mu_{\tilde{A}_i(f_i')}(u_i)$ of the GT2FS $\tilde{A}_i$, the following strategies are adopted.

1. Let, $\mu_{\tilde{A}_i(f_i')}(u_i)$ be the secondary membership of the *i*-th antecedent proposition defined at the linguistic value $f_i = f_i'$, and primary membership u_i, where u_i is sampled at uniform interval ends: $u_{i,1}, u_{i,2}, ..., u_{i,m}$ for *i* = 1 to *n*. Here, $u_i = u_{i,p} = \underline{u}_i = \underline{\mu}_{\tilde{A}_i}(f_i')$ and $u_i = u_{i,q} = \bar{u}_i = \bar{\mu}_{\tilde{A}_i}(f_i')$ are the two extremities of the FOU over $f_i = f_i'$. Here *m* is the used-defined positive integer (optimized in the present application.)
2. The secondary membership $\mu_{\tilde{A}_i(f_i')}(u_i)$ would have a peak at the center of $[\underline{u}_i, \bar{u}_i]$, as the uncertainty is minimum at the center, where, $m_i = (\underline{u}_i + \bar{u}_i)/2$.
3. The secondary membership here defined as

$$\mu_{\tilde{A}_i(f_i')}(u_i) = \exp[-\frac{(u_i - m_i)^2}{2\sigma_i^2}] \qquad (19)$$

where, $u_i = [u_{i,p}, u_{i,q}] = [\underline{u}_i, \bar{u}_i]$, for $f_i = f_i'$ and σ_i^2 is a user defined parameter. The value of σ_i^2 is obtained by an optimization algorithm given in section III.

C. General Type-2 Fuzzy Reasoning used in the Training Phase

Let $f_1 = f_1', f_2 = f_2', ..., f_n = f_n'$ be a measurement point. The secondary grade of membership $\mu_{\tilde{A}_i(f_i)}(u_i)$ at $f_i = f_i'$ is a vertical slice, represented by a Gaussian MF, given by (19).

The following steps are adopted for the assessment of perceptual-degradation of the olfactory stimulus.

1. Generally, the secondary MFs in a GT2FS provide information about the degree of correctness of the primary membership assignments. Thus given a secondary MF $\mu_{\tilde{A}_i(f_i')}(u_i)$ it can be utilized to refine the primary memberships value $u_{i,k}$ at $f_i = f_i'$, for *k* = 1 to *m* and *i* = 1 to *n* by a suitable mapping function (illustrated in Fig. 7). Expression (20) provides one such mapping function from secondary $\mu_{\tilde{A}_i(f_i')}(u_i)$ to refined primary membership values $p_{i,k}$. Let the modified primary membership value at (f_i', u_i) be $p_{i,k}$, where,

$$p_{i,k} \leftarrow u_{i,k}^{1-\mu_{\tilde{A}_i(f_i')}(u_{i,k})}. \qquad (20)$$

Thus for a given $u_{i,k}$, we have a corresponding $p_{i,k}$ along the $f_i = f_i'$ axis.

It is noteworthy, that the refined primary membership value $p_{i,k}$ is more strengthened by powering the original primary membership function (MF) by complement of the secondary MF at the given (f_i', u_i). The mapping function (20) ensures that the width of the FOU is reduced (hard line in Fig.7) in comparison to its pre-constructed width at given measurement point $f_i = f_i'$.

2. For $u_{i,k} \in [\underline{u}_i, \bar{u}_i]$, a set $P_i = \{p_{i,k} : 1 \le k \ge m\}$, respectively the refined primary membership values lying in the FOU, is computed. The *Refined-UMF* (UMF_{Re}) ($P_i^{\max}$) and *Refined-LMF* (LMF_{Re}) ($P_i^{\min}$) of $\tilde{A}_{i_{\mathrm{Re}}}(f_i)$ at $f_i = f_i'$, are obtained as

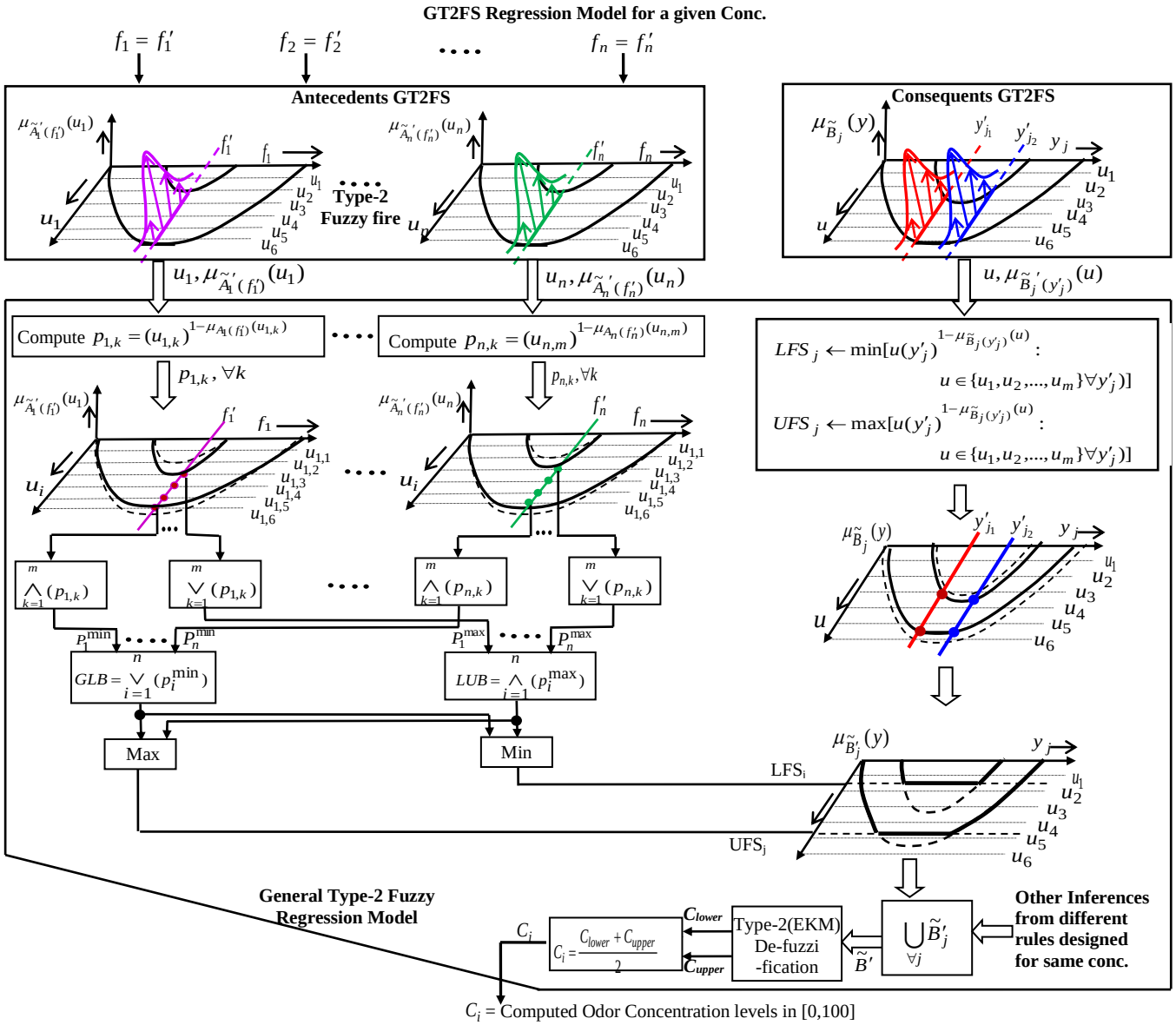

Fig.7. Architecture of the proposed General Type-2 Fuzzy regression model for a fixed concentration

$$UMF_{\mathrm{Re}} = P_i^{\max} = \bigvee_{k=1}^{m} \{p_{i,k}\}, \quad (21)$$

$$LMF_{\mathrm{Re}} = P_i^{\min} = \bigwedge_{k=1}^{m} \{p_{i,k}\}, \quad (22)$$

where, $\bigvee_{k=1}^{m}$ and $\bigwedge_{k=1}^{m}$ denote the cumulative OR (max) and AND (min) operator operators respectively.

3. Step 2 is repeated to obtain $UMF_{\mathrm{Re}}: P_1^{\max}, P_2^{\max}, ..., P_n^{\max}$ and LMF_{Re}: $P_1^{\min}, P_2^{\min}, ..., P_n^{\min}$ for the refined fuzzy sets $\tilde{A}_{1_{\mathrm{Re}}}(f_1), \tilde{A}_{2_{\mathrm{Re}}}(f_2), ..., \tilde{A}_{n_{\mathrm{Re}}}(f_n)$ respectively.

4. The *Least Upper Bound (LUB)* of the UMF_{Re}: $P_1^{\max}, P_2^{\max}, ..., P_n^{\max}$ of the refined fuzzy sets is obtained by

$$LUB = P_1^{\max} \wedge P_2^{\max} \wedge ... \wedge P_n^{\max} = \bigwedge_{i=1}^{n} P_i^{\max}. \quad (23)$$

Similarly, the *Greatest Lower Bound (GLB)* of the LMF_{Re}: $P_1^{\min}, P_2^{\min}, ..., P_n^{\min}$ of the refined fuzzy sets is obtained by

$$GLB = P_1^{\min} \vee P_2^{\min} \vee ... \vee P_n^{\min} = \bigvee_{i=1}^{n} P_i^{\min}. \quad (24)$$

5. *The Upper Firing Strength (UFS)* and the *Lower Firing Strength (LFS)* of rule *j*, given by UFS_j and LFS_j are obtained as

$$LFS_j = Min(LUB, GLB), \quad (25)$$

$$UFS_j = Max(LUB, GLB). \quad (26)$$

D. GT2FS Based Type-2 Fuzzy Inference Generation

The fuzzy reasoning module attempts to derive type-2 fuzzy inference y is $\tilde{B}_j$, indicating the odor concentration levels present in the aromatic substance experienced by a subject.

The parameter y is defined as the centre value of the grade specified by the subject in his/her oral response, after examining a given stimulus.

The following steps are executed to compute the Lower firing strength (LFS) and upper firing strength (UFS) for rule *j*.

a) Compute a set S_j containing the modified primary membership $u(y'_j)$ and the secondary MF $\mu_{B_j(y'_j)}(u)$ at $y_j = y'_j \in Y_j$ as its elements (Fig. 7).

$$s_j = \{u(y'_j)^{1-\mu_{\tilde{B}_j(y'_j)}(u)} \Big| u \in J_{y_j} = \{u_1, u_2, ..., u_m\} \subseteq [0,1], \text{ for } y_j = y'_j, \forall y_j \in Y_j\} \quad (27)$$

b) Select positive elements of set S_j (by dropping zero elements) and call the resulting set S'_j.

$$S'_j = \{s_j \in S_j \mid s_j > 0\} \quad (28)$$

c) Obtain LFS_j of Rule $_j = s_k$, where $s_k \le s'_j \in S'_j$.

d) Obtain UFS_j of Rule $_j = s_l$, where $s_l \ge s'_j \in S'_j$.

6. Let $\mu_{\tilde{B}_j}(y)$ be an IT2MF representing rule *j* of linguistic variable *y*. The following transformation is used to obtain the resulting IT2MF $\tilde{B}'_j = [\underline{\mu}_{\tilde{B}'_j}, \overline{\mu}_{\tilde{B}'_j}]$, where

$$\underline{\mu}_{\tilde{B}'_j} = \min\ (LFS_j, \underline{\mu}_{\tilde{B}_j}) \quad (29)$$

and

$$\overline{\mu}_{\tilde{B}'_j} = \min\ (UFS_j, \overline{\mu}_{\tilde{B}_j}) \quad (30)$$

7. In case there exist multiple rules, we take the union of the type-2 fuzzy interfaces, given by

$$\mu_{\tilde{B}'} = \bigcup_{\forall j} \mu_{\tilde{B}'_j}, \quad (31)$$

which is computed by the following 2 steps.

$$\overline{\mu}_{\tilde{B}'} = \max_{\forall j} (\overline{\mu}_{\tilde{B}'_j}) \quad (32)$$

$$\underline{\mu}_{\tilde{B}'} = \min_{\forall j} (\underline{\mu}_{\tilde{B}'_j}) \quad (33)$$

8. Karnik-Mendel (KM) defuzzification [48] is used next to evaluate the left and right end point centroids. Any version of KM algorithm would serve the purpose. However, the Enhanced KM (EKM) algorithm is used here to minimize the computational overhead. After obtaining the left end point centroid (C_{lower}) and the right end point centroid (C_{upper}), the centroid (C_i) is computed by taking the average of C_{lower} and C_{upper} [49]

$$C_i = \frac{C_{lower} + C_{upper}}{2} \quad (34)$$

Here, the centroid C_i is represented as the measure of odor concentration levels of a given smell stimulus experienced by the subject in [0, 100] scale.

E. Optimal Selection of σ_i

The secondary membership functions of the linguistic variables used in the antecedent propositions of the fuzzy rules are initially selected as Gaussian memberships with peak at the centre of the FOU. However, in order to train the type-2 fuzzy regression model with a list of training instances, including antecedent features $f_1, f_2, ..., f_n$ and corresponding subject-produced grades of concentration, the secondary memberships need to be adjusted. Fig. 9 provides a schematic overview of standard deviation selection of secondary memberships by an evolutionary algorithm. The objective here is to optimally select the secondary membership standard deviations of the antecedent proposition to establish the antecedent variables to consequent regression. This is done by the following steps.

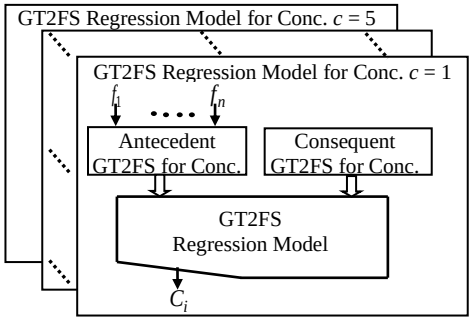

Fig.8. GT2FS Regression Model for different Concentration levels of a single odor

First, run the type-2 fuzzy regression algorithm *n* times for *n* set of training instances and thus to produce *n* error values E_1 through E_n, with $E_i = D_i - C_i$, where D_i and C_i respectively are the desired and the computed odour concentration provided by the subject. Second, the E_i s for *i* =1 to *n* are buffered to compute $J = (\sum_{i=1}^{n} E_i^2)^{1/2}$. Third, a meta-heuristic algorithm is employed to minimize *J* with an aim to judiciously select the secondary membership parameters: $\sigma_1, \sigma_2, ..., \sigma_n$. Although any meta-heuristic algorithm can be employed to optimize *J*, DE is used to serve the purpose. Finally, the optimal standard deviations of the secondary memberships thus obtained are $\sigma_1^o, \sigma_2^o, ..., \sigma_n^o$.

F. Optimal Parameter Selection of GT2FS Regression Model

Fig.10 provides a schematic overview of the complete system during the training phase with special emphasis to 2 feedback loops, one to adapt variance of secondary membership functions, and the outer feedback loop is to adapt discretization parameter *m* and one parameter η used in feature selection. The principles of selection of *m* and η are explained in the Grid search algorithm [31] presented in Table I. The algorithm attempts to vary *m* and η in user-defined intervals $[m_{\min}, m_{\max}]$ and $[\eta_{\min}, \eta_{\max}]$ and increments δm and $\delta\eta$ respectively and compute *J* for each (m, η) and then finds the optimal *m* and η represented as m_{opt} and η_{opt}, respectively that minimizes $J(m,\eta)$. The optimal values of the overall model parameters obtained for the GT2FS regression are: $\eta = 0.056$ and m = 6. Fig. 2 in the Appendix A.4 [65] provides a 3D plot of $J(m,\eta)$ against m and η, indicating that an off-tune from the optimal settings of η and *m* yields a steep rise in $J(m,\eta)$, ensuring the

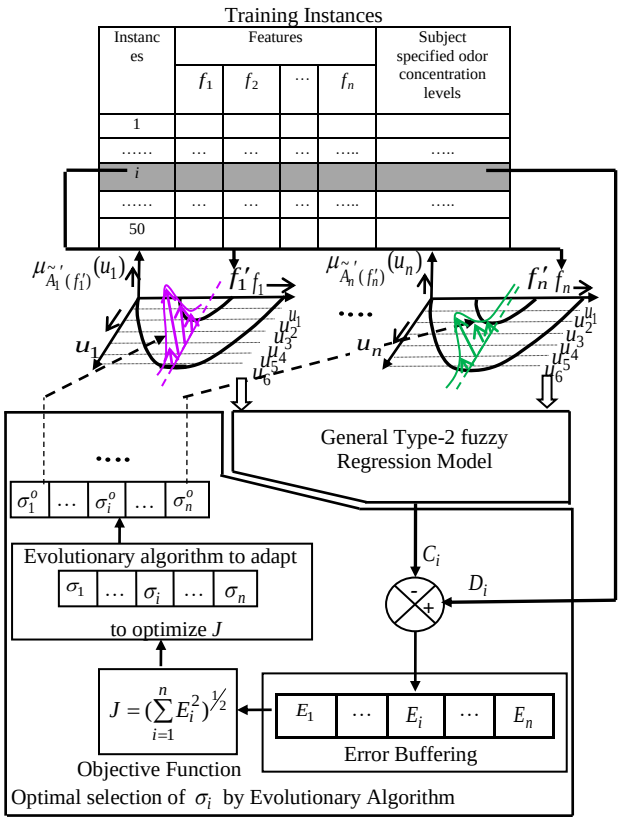

Fig.9. Optimal Selection of standard deviations σ_i of Secondary Membership Function

TABLE-I PSEUDO CODE OF GRID SEARCH ALGORITHM

Grid-search (m,η)

1. **For** each pair of (m,η), where $m \in [m_{\min}, m_{\max}]$ and $\eta \in [\eta_{\min}, \eta_{\max}]$ with pre-defined increments δm and $\delta\eta$, undertake Type-2 fuzzy regression and computation of $J = (\sum_{i=1}^{n} E_i^2)^{1/2}$
2. Save $J(m,\eta)$ in a 2-dimentional array of (m,η).
3. **End_For**;
4. Search the smallest $J=J_{min}$ for $m \in [m_{\min}, m_{\max}]$ and $\eta \in [\eta_{\min}, \eta_{\max}]$. Let $J(m,\eta) = J_{\min}$ for $m = m_{opt}$ and $\eta = \eta_{opt}$.
5. Assign $m \leftarrow m_{opt}$ and $\eta \leftarrow \eta_{opt}$.
6. Print (m,η).

optimality of $J(m,\eta)$ at $\eta = 0.056$ and m = 6.

Time-complexity: The computation of the UFS and LFS is undertaken in 2 steps. In the first step, we compute $P_i^{\max}$ and $P_i^{\min}$ respectively by (21) and (22), which require a complexity of $O(m)$. In the next step, we compute LUB and GLB by (23) and (24) respectively, that require a complexity of $O(m.n)$ [50]. Here, n denotes the number of linguistic variables in the antecedent, and m denotes the number of discretization along the u_i axis. Again for computation of LFS and UFS respectively by (25) and (26), an additional complexity of $O(n)$ is required. Finally, for v discretization in the y-axis (consequent side), a total complexity of $O(v)$ is required to generate the type-2 inference. So, the overall complexity = $O(m.n) + O(n) + O(v)$, which effectively boils down to $O(m.n)$ as n and $v << m.n$.

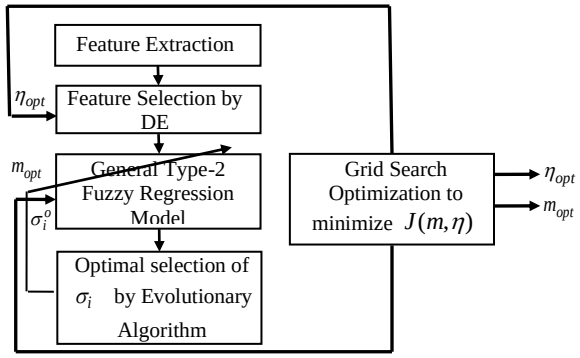

Fig.10. Computation of optimal parameters η_{opt} and m_{opt} using grid-search algorithm

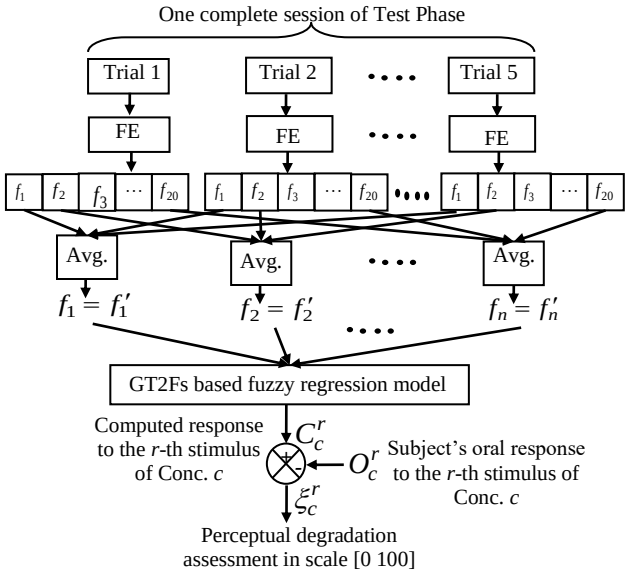

Fig.11. Perceptual degradation assessment of a subject during test phase

G. Test phase

The olfactory perceptual model of the subject built up in the training phase is used in the test phase to determine his/her degree of olfactory degradation. In the test phase, we need to extract the features $f_1, f_2, ..., f_n$ from the acquired hemodynamic response to pre-calibrated olfactory stimuli to use them as the input of the perceptual model of the subject. The model response (that represents the subject's judgement about odour concentration during the training period) is now compared with subject's current oral response about odour concentration. The difference between the above 2 concentration values represents a quantitative measure of the subject's possible degradation in olfactory perception. To avoid the possible infiltration of measurement noise in the features, in Fig. 11, we arranged 5 trials of stimulus presentation, fNIRs pre-processing, and extraction of selected 20 features over each trial. Then the average value of features over 5 trials is taken as indicated in Fig. 11 and submitted to GT2FS regression model for evaluation of predicted oral response of the subject.

Let ξ_c^r be a measure of the olfactory perceptual degradation of a given subject to a calibrated olfactory stimulus r with a given concentration c, represented as,

$\xi_c^r = | C_c^r - O_c^r |$, where, C_c^r represents the model response in [0, 100] and O_c^r is the centre value of the grade specified by the subject in her oral response. The root mean square error (RMSE) of ξ_c^r for c = 1 to b concentration levels of stimulus r, is given by

$$RMSE^r = (\sum_{c=1}^{b} (\xi_c^r)^2 / b)^{1/2}. \quad (35)$$

The average value of the RMSEs across all the stimuli used is obtained by

$$\overline{RMSE} = \sum_{r=1}^{R} RMSE^r / R. \quad (36)$$

Now, the Olfactory Perceptual Degradation (OPD) of a subject in percentage is evaluated by

$$OPD = (\frac{\overline{RMSE}}{{}^{Max}\overline{RMSE}_{th} - {}^{Min}\overline{RMSE}_{th}}) \times 100, \quad (37)$$

where, ${}^{Max}\overline{RMSE}_{th}$ be the theoretical maximum value of $\overline{RMSE}$ and ${}^{Min}\overline{RMSE}_{th}$ be the theoretical minimum value of $\overline{RMSE}$.

IV. Experiments And Results

This section aims at designing the following experiments of the prediction of olfactory perceptual-degradation using f-NIRs device.

A. fNIRs data acquisition and List of Odor stimulus

The experiment has been performed in Artificial Intelligence laboratory of Jadavpur University, Kolkata, India [51]. Here, a whole brain f-NIRs (NIRScoutTM imager) system is used to capture the hemodynamic response of the brain. The f-NIRs device is manufactured by NIRx Medical Technologies LLC, with 8 infrared (IR) sources and 8 infrared detectors are placed over the scalp of the subjects according to the international 10-10 system. Here 8 source and 8 detectors forms 8 × 8 = 64 channels, of which 20 channels are selected followed by nearest neighboring source-detector combinations according to 10-10 placement system. In the present application, a set of 10 distinct smell stimuli (Rose water, Male perfume, Phenyl, Clove oil, Lavender oil, Kerosene oil, Camphor oil, Eucalyptus oil, Liquid Hydrogen sulfide, and Ammonium Hydroxide) with 5 different concentration levels are used to measure the olfactory perceptual-degradation of a subject.

B. Participants

30 volunteers, in the age group of 20-45 years, were allowed to participate in the experiment [51] after obtaining their written consent. Ethical issues and all other safety measures were maintained as per Helsinki declaration of 1970, revised in 2004 [52]. The participants include a healthy group of 22 volunteers (HS1-HS22), and a diseased group of 8 volunteers. The latter group comprises 4 patients suffering from Alzheimer's disease (DS1-DS4), 3 carrying Hyposmia (indicating reduced ability to detect odors) Olfactory Disorder (DS5-DS7), and one carrying Parosmia (having inability to detect distorted odors) Olfactory Disorder (DS8). Each subject is instructed to take a comfortable resting position to avoid possible pick-ups of muscles artifacts.

C. Experiment 1: Subject familiarity with stimulus concentration

The following steps are employed to get the subjects familiarized with the relative concentration levels of the stimuli presented for a given odor.

1. Ask the subject to concentrate on the computer monitor on a fixation cross for 3S.
2. Submit an odor of preselected concentration for 5S with a delay of 2 minutes.
3. Repeat step 2 for the same odor of different concentration.
4. After presentation of stimuli of the same odor of 5 different concentration levels are over, ask the subject to qualify the 5 stimuli into one of 5 grades: Very Low, Low, Medium, High and Very High based on their relative concentration levels.
5. Represent the actual concentrations of the stimuli presented in [0, 100], and obtain the measure of grades of the stimuli as Very Low, Low, Medium, High, Very High based on the measure of the estimated concentration respectively in [1, 20), [20, 40), [40, 60), [60, 80), [80, 100] ranges.
6. Match the grades of 5 concentration levels presented by the subject in his oral response with those obtained in step 5. In case the labels of all the 5 concentrations are correct, stop, else repeat from step 1.

The above steps are repeated for 10 distinct odors, each of 5 concentration grades, indicated above, with a delay of 5 minutes between presentations of two successive odors.

D. Experiment 2: Identification of active brain regions for different concentration levels

This experiment attempts to identify the brain regions responsible for decoding of concentration levels of the olfactory stimulus (clove oil) at best three different concentration levels, one falling in the very low grade, one in the medium and one in the very high grade. Here, nirsLAB software has been used to get the mean HbO concentration over the 22 channels respectively. It is noted that for healthy subjects, the oxygen consumption in pre-frontal lobe is highly increased during the perception of various concentration level of olfactory stimulus. The hemodynamic load distribution in the pre-frontal cortex before presenting the olfactory stimulus is shown in Fig. 12 (a). The maximum activation for concentration 1, 3 and 5 are depicted in Fig. 12 (b), 12 (c) and 12 (d) respectively. The corresponding changes in the topographic map are listed below.

1. Initially, the hemodynamic load distribution takes place in the pre-frontal region during perceiving an odor stimulus (clove oil) with its fixed concentration.
2. The activation shifts to the Orbito frontal cortex (OFC) after perceiving first (very Low) concentration level. Additionally, small changes in concentration level initiates activation in Boardmann area 10, 11 which have a functions in olfactory signal processing and perception [53].
3. The activation of the orbito frontal cortex (OFC) is reduced gradually with increased concentration of the aromatic stimulus from Conc. 1 (Very low) to Conc. 3 (Medium).

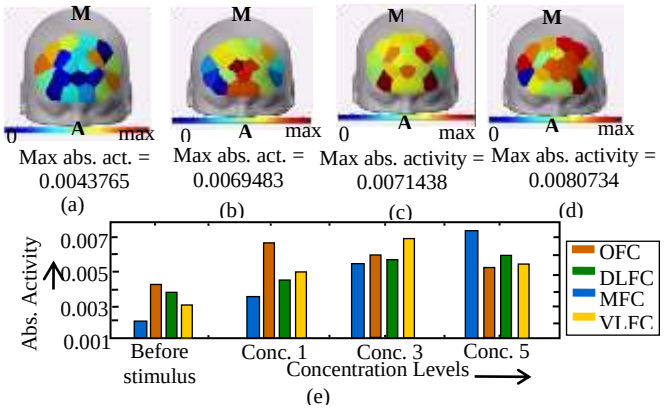

Fig.12. Topographic maps of the oxy hemoglobin concentration for (a) before application of aromatic stimulus, (b) odor concentration (Conc.) level 1, (c) odor concentration level 3, (d) odor concentration level 5, (e) Quantitative measure of oxygen consumption in the pre-frontal (frontal) lobe with increasing concentration of the odor stimulus

Moreover, the cortical activation pattern spread to Dorso lateral pre-frontal cortex and vento-lateral pre-frontal cortex.

4. Finally, with increase in concentration of the aromatic substance at Conc. 5 (Very high), the activation of the Pre-frontal cortex is shifted to frontal region. The middle frontal cortex has the broader activation compared to the pre-frontal cortex. The quantitative measures of the above implications have been produce in Fig. 12 (e) to maintain the consistency of the data. It is also noted that subjects with olfactory disorder, occasionally fail to recognize the concentration of the given stimuli at the expected brain regions.

E. Experiment 3: Subjective Sensitivity Analysis from the Hemodynamic response

Sensitivity in engineering refers to the weakest possible signal that a machine can measure [54]. Here, the sensitivity of subjects is compared with reference to the measure of normalized oxygen consumption (NOC), averaged over an interval of time (ANOC), starting from the onset of the stimulus. The definition of ANOC is given in eq. (38).

$$ANOC = \sum_{t=t_0}^{t_0+T} \hat{d}_{\phi}(t) \Big/ T, \tag{38}$$

where, t_0 and T be the starting and end time points. Fig. 13 provides a plot of the ANOC with respect to concentration variation to have an idea of sensitivity of the subjects to stimuli of varied concentrations. It is noted from the plot that the persons with brain diseases have relatively lower values in ANOC for stimulus of very low, low and medium concentrations, in comparison to those of healthy individuals. The experiment thus ensures that subjects with olfactory disorder have lower sensitivity than the healthy subjects.

F. Experiment 4: Olfactory Perceptual Degradation (OPD) Assessment of a subject during test phase

The prime motivation of this experiment is to determine the degradation of olfactory perception for both healthy and diseased subject in the test phase. It is clear from Fig. 14, that the olfactory degradation is very high for diseased subject 3 whereas it is least for healthy subject 3. Here, the subjects are ranked in the ascending order of their OPDs. The following conclusions are drawn from the experiment.

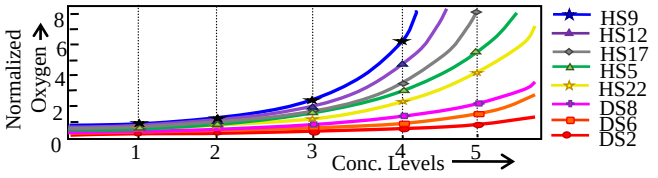

Fig. 13 Average normalized Oxygen Consumption (ANOC) versus Conc. variation plot. The non-intersecting curves only are selected for clarity

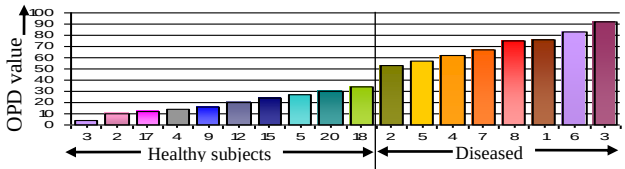

Fig.14. Olfactory perceptual disorder assessment of healthy and diseased subjects according to their ranks

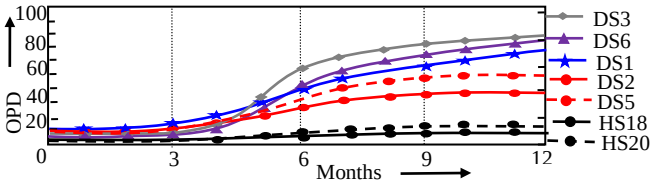

Fig.15. monthly OPD measurements for 2 healthy subjects and 5 diseased subjects

1. The OPD results provide a clear demarcation between the healthy and the diseased subjects.
2. It is noted that OPD increases for people with olfactory disorder. A relatively higher OPD for healthy people indicates a tendency towards acquiring olfactory disorder.

G. Experiment 5: Validation of OPD by Monthly Assessment

In order to examine the performance of the proposed GT2FS based regression model, a monthly assessment of olfactory disorder is carried out by measuring monthly OPD over one year after completion of subject training. It is noted that for healthy subjects, the monthly variation is ignorable, whereas for persons with olfactory disorders exhibit a gradual degradation in OPD measure. Fig. 15 depicts the results of monthly OPD measurements for 2 healthy subjects and 5 diseased subjects only (to avoid clumsiness). It is evident from Fig 15, that perceptual degradation of healthy subject has little variation around zero value. On the other hand, for olfactory diseased persons, the perceptual degradation measure increases over months.

V. Performance Analysis and Statistical Evaluation

This section compares the performance of the proposed General Type-2 fuzzy regression with the state-of-the-art techniques. This is done with reference to the value of percentage success rate (PSR), run-time complexity and statistical test. Here, for each subject, there are 25 training instances in a session for a given odor sample of a fixed concentration level. Again for 10 different odor samples, we have 25 × 10 = 250 instances. These 250 instances together constitute one dataset for individual subject. Similarly, for 30 subjects, we have 30 distinct datasets. The 30 datasets, each of 250 instances, are presented in separate folders in the URL given in [64], [65].

TABLE-II
COMPARISON OF AVERAGE PSR OBTAINED BY THE PROPOSED REGRESSION METHOD AGAINST EXISTING METHODS ACROSS 30 DATASETS

Existing Reasoning Algorithm with optimal settings of parameters	**Avg. PSR**	**Run-time in IBM PC Dual-core Machine**
Regression using LSVM [55]	78.9%	56.28 milliseconds
Regression using SVM with Gaussian Kernel [56]	80.7%	57.76 milliseconds
BPNN based Regression [57]	74.1%	62.37 milliseconds
Polynomial Regression of order 10	72.6%	104.25 milliseconds
Genetic Algorithm induced Type-I Fuzzy regression [59]	66.2%	46.28 milliseconds
Differential Evolution (DE) Induced IT2FS regression [60]	85.6%	45.71 milliseconds
TSK model [61] extended for GT2FS regression	87.2%	95.48 milliseconds
GT2FS based regression [62]	89.6%	95.12 milliseconds
Proposed GT2FS model	**96.3%**	**94.78 milliseconds**

TABLE III
ORDER OF COMPLEXITY OF THE PROPOSED METHOD WITH OTHER GT2FS ALGORITHMS

GT2FS Based Reasoning Methods	Order of Complexity
Proposed GT2FS	$O(m.n)$
Vertical slice based GT2FS [28]	$O(m^n)$
Z-slice Based GT2FS [27]	$O(m.n.I)$
Z-slice Based GT2FS [50]	$O(m.n.I)$

Let, C_i and D_i be the computed and desired odor concentration level for i-th training instance obtained from the oral response of the subject. Now, to calculate the success rate for each data set, first, we identify the successful instances for each dataset by satisfying the chosen inequality criterion: $[D_i - 5\%\ of\ D_i] \le C_i \le [D_i + 5\%\ of\ D_i]$ (Appendix A.2 [65]). Second, for all the 250 instances in each dataset Percentage Success rate (PSR) is evaluated by,

$$PSR = \frac{\text{No of successful intances}}{250} \times 100. \qquad (39)$$

Next, average PSR of each algorithm is obtained by taking the PSR obtained from 30 different datasets for the same algorithm.

A. *Performance Analysis of the proposed GT2FS reasoning methods*

To evaluate the relative performance of the proposed type-2 fuzzy reasoning method with the existing techniques, we undertake PSR and the runtime complexity for comparison. Table-II provide the results of PSR obtained by the proposed type-2 fuzzy set based regression techniques against traditional type-1 [59], type-2 fuzzy algorithms [60]- [62] and non-fuzzy regression algorithm including L-th order of polynomial regression [58], Linear support vector machine (SVM) based regression [55], SVM with Gaussian kernel [56], Back propagation neural network (BPNN) based regression [57], realized and tested for the present perceptual task. The optimal parameter sets of all the algorithms are included in Table- IV (Appendix A.3 [65]). It is apparent from Table-II that the proposed reasoning algorithm outperforms its nearest competitors by a large margin. It is also observed form the same table that the runtime complexity of the proposed GT2FS algorithm is 94.7 milliseconds, which is comparably less than the other existing GT2FS based techniques.

B. *Computational Complexity Analysis of the proposed GT2FS Method*

To determine the computational performance analysis of the Type-2 Fuzzy reasoning, we evaluate order of complexity in terms of total number of t-norm, and s-norm computations [50]. Table-III provides the results of run-time complexity analysis to demonstrate that the order of complexity of the proposed algorithm is significantly less than its competitors. In Table-III, n is the number of selected features, m is the number of discretization levels along the y-axis and I is the number of z-slices, considered in GT2FS based algorithms.

C. *Statistical validation with Friedman Test*

The Friedman test [63] is used here to statistically compare the performance of the proposed algorithm with respect to 8 other well-known algorithms and 30 datasets of 250 instances. The rank of individual algorithm for each dataset is evaluated using the PSR metric defined earlier. The detailed computation of ranking of the algorithms is given in Appendix A.2 [65]. The χ_F^2 is evaluated based on the average rank of individual algorithms over 30 datasets. It is noted that the computed $\chi_F^2 > \chi^2_{(9-1),0.95}$, the value obtained from chi-sqr table for 8 degrees of freedom at 95% confidence level. The above criterion ensures that the null hypothesis, claiming that all the chosen algorithms have identical performance, is wrong, and thus rejected, thereby justifying the rank estimation of the algorithms by the PSR metric.

VI. CONCLUSION

The paper introduced a new technique for olfactory perceptual degradation assessment of human subjects using an f-NIRs device. Experimental analysis undertaken confirms that the proposed model can detect possible olfactory perceptual degradation over months, particularly for subjects with olfactory disorder. A run-time complexity analysis envisages that the proposed algorithm outperforms its competitors by a large margin. A Friedman test confirms better statistical performance of the proposed technique with its competitors to a confidence level 95%.

REFERENCES

[1] G. A. Wright and B. H. Smith, "Variation in complex olfactory stimuli and its influence on odour recognition. Proceedings of the Royal Society of London," *Series B: Biological Sciences*, vol. 271, no.1535, pp. 147-152, 2004.

[2] J. L. Schwartz, N. Grimault, J. M. Hupé, B. C. Moore, and D. Pressnitzer, "*Multistability in perception: binding sensory modalities, an overview*," 2012.

[3] B. Schaal, K. Durand, *The role of olfaction in human multisensory development. Multisensory development*, pp. 29-62, 2012.

[4] J. Kum *et al*, "Neural dynamics of olfactory perception: low-and high-frequency modulations of local field potential spectra in mice revealed

by an oddball stimulus," *Frontiers in neuroscience*, vol. 13, pp. 478, 2019.

[5] S. R. Jaeger, J, F. McRae, C. M. Bava, M. K. Beresford, D. Hunter, Y. Jia, and K. R. Atkinson, "A Mendelian trait for olfactory sensitivity affects odor experience and food selection. Current Biology," vol. 23, no.16, pp. 1601-1605, 2013.

[6] Li Mo and Liu Yunhao "Underground coal mine monitoring with wireless sensor networks*," ACM Trans. on Sensor Networks (TOSN)*, vol. 5, no. 2, 2009.

[7] P. Dalton, B. Cowart, D. Dilks, M. Gould, P. S. Lees, A. Stefaniak, and E. Emmett, "Olfactory function in workers exposed to styrene in the reinforced-plastics industry," *American journal of industrial medicine*, vol. 44, no. 1, pp. 1-1, 2003.

[8] N. A. Martínez, G. A. Carrillo, P. S. Alvarado, C. M, García, A. V. Monroy and F. V. Campos, "Clinical importance of olfactory function in neurodegenerative diseases," *Revista Médica del Hospital General de México*, vol. 81, no.4, pp.268-275, 2018.

[9] C. Murphy, M. M. Gilmore, C. S. Seery, D. P. Salmon, and B. R. Lasker,"Olfactory thresholds are associated with degree of dementia in Alzheimer's disease," *Neurobiology of aging*, vol. 11, no. 4, pp. 465-469,1990.

[10] C. Wu, J. Liu, P. Zhao, M. Piringer, and G. Schauberger, "Determination of the Odour Concentration and Odour Intensity of a Mixture of Odorous Substances by Chemical Concentrations: a Comparison of Methods," *Chemical Engineering Trans.*, vol. 54, pp. 97-102, 2016.

[11] K. D. Foster, J. M. Grigor, J. N. Cheong, M. J. Yoo, J. E. Bronlund, and M. P. Morgenstern, "The role of oral processing in dynamic sensory perception.," *Journal of Food Science*, vol. 76, no. 2, pp. R49-R61, 2011.

[12] H. Harada, M. Tanaka, and T. Kato, "Brain olfactory activation measured by near-infrared spectroscopy in humans," *The Journal of Laryngology & Otology*, vol. 120, no. 8, pp. 638-643, 2006.

[13] K. Azuma, I. Uchiyama, M. Tanigawa, I. Bamba, M. Azuma, H. Takano and K. Sakabe, "Assessment of cerebral blood flow in patients with multiple chemical sensitivity using near-infrared spectroscopy—recovery after olfactory stimulation: a case–control study," *Environmental health and preventive medicine*, vol. 20, no. 3, pp.185, 2015.

[14] S. Fazli, J. Mehnert, J. Steinbrink, G. Curio, A. Villringer, K. R. Müller and B. Blankertz, "Enhanced performance by a hybrid NIRS–EEG brain computer interface," *Neuroimage*, vol. 59, no. 1, pp. 519-529, 2012.

[15] Y. Nagata, and N. Takeuchi, "Measurement of odor threshold by triangle odor bag method," *Odor measurement review*, vol.*118*, pp. 118-127, 2003.

[16] J. P. Lehrner, J. Glück and M. Laska, "Odor identification, consistency of label use, olfactory threshold and their relationships to odor memory over the human lifespan," *Chemical Senses*, vol. 24, no. 3, pp. 337-346, 1999.

[17] M. R. Woodward *et al*., "Validation of olfactory deficit as a biomarker of Alzheimer disease," *Neurology: Clinical Practice*, vol. 7, no. 1, pp. 5-14, 2017.

[18] Y. M. Zou, Da Lu, L. P. Lui, H. H. Zhang, and Y. Y. Zhou, "Olfactory dysfunction in Alzheimer's disease," *Neuropsychiatric disease and treatment*, vol. 12, pp.869, 2016.

[19] G. Placidi, A. Petracca, M. Spezialetti, and D. Iacoviello, "Classification strategies for a single-trial binary Brain Computer Interface based on remembering unpleasant odors," *37th Annual International Conference of the IEEE Engineering in Medicine and Biology Society (EMBC)* , pp. 7019-7022. IEEE, 2015.

[20] A. Saha, A. Konar, A. Chatterjee, A. L. Ralescu & A. K. Nagar, "EEG analysis for olfactory perceptual-ability measurement using recurrent neural classifier," *IEEE Trans. Human-machine systems*, vol. 44, no. 6, pp. 717-730, Dec. 2014.

[21] D. A. Wilson, and R. J. Stevenson, 2003). "The fundamental role of memory in olfactory perception," *Trends in neurosciences*, vol. 26, no. 5, pp. 243-247, 2003.

[22] M. Schecklmann *et al*., "Altered frontal and temporal brain function during olfactory stimulation in adult attention-deficit/hyperactivity disorder," *Neuropsychobiology*, vol.63, no. 2, pp. 66-76, 2011.

[23] L. Ghosh, A. Konar and P. Rakshit, *Cognitive Modeling of Human Memory and Learning: A Non-invasive Brain-Computer Interfacing Approach*, John Wiley & Sons, 2020.

[24] M. Ferrari and V. Quaresima, "A brief review on the history of human functional near-infrared spectroscopy (fNIRS) development and fields of application," *Neuroimage*, vol. 63, no. 2, pp. 921-935, 2012.

[25] J. M. Mendel, H. Hagras, W. W. Tan, W. W. Melek, and H. Ying, *Introduction to type-2 fuzzy logic control: theory and applications*, John Wiley & Sons, 2014.

[26] D. Wu, "On the fundamental differences between interval type-2 and type-1 fuzzy logic controllers*," IEEE Trans. on Fuzzy Systems*, vol. 20, no. 5, pp. 832-848, 2012.

[27] J. M. Mendel, "General type-2 fuzzy logic systems made simple: a tutorial." *IEEE Trans. Fuzzy Systems*, vol. 22, no. 5, pp. 1162-1182, 2014.

[28] J. M. Mendel, I. J. Robert, and L. Feilong, "Interval type-2 fuzzy logic systems made simple," *IEEE Trans. Fuzzy Systems*, vol. 14, no. 6, pp. 808-821, 2006.

[29] J. M. Mendel, M. R. Rajati and P. Sussner, "On clarifying some definitions and notations used for type-2 fuzzy sets as well as some recommended changes", *Information Sciences*, pp. 337-345 , 2016

[30] J. H. Aladi, C. Wagner, and J. M. Garibaldi, "Type-1 or interval type-2 fuzzy logic systems—On the relationship of the amount of uncertainty and FOU size," *IEEE international conference on fuzzy systems (FUZZ-IEEE)*, pp. 2360-2367. IEEE, 2014.

[31] M. Ataei, and M. Osanloo, "Using a combination of genetic algorithm and the grid search method to determine optimum cutoff grades of multiple metal deposits," *International Journal of Surface Mining, Reclamation and Environment*, vol. 18, no. 1, pp: 60-78, 2004.

[32] M. Xu, Y. Minagawa, H. Kumazaki, K. I. Okada, and N. Naoi, "Prefrontal Responses to Odors in Individuals With Autism Spectrum Disorders: Functional NIRS Measurement Combined With a Fragrance Pulse Ejection System," *Frontiers in human neuroscience*, vol. 14, pp. 432, 2020.

[33] Amiyangshu De, Mousumi Laha, Amit Konar, Atulya K. Nagar, "Classification of Relative Object Size from Parietooccipital Hemodynamics Using Type-2 Fuzzy Sets,"*FUZZ-IEEE*, pp: 1-8, 2020.

[34] M. Laha, A. Konar, P. Rakshit, L. Ghosh, S. Chaki, A. L. Ralescu, and A. K. Nagar, "Hemodynamic Response Analysis for Mind-Driven Type-writing using a Type 2 Fuzzy Classifier," *IEEE International Conference on Fuzzy Systems (FUZZ-IEEE)*. pp. 1-8). IEEE, 2018.

[35] N. Naseer, and K. S. Hong, "fNIRS-based brain-computer interfaces: a review," *Frontiers in human neuroscience*, vol. 9, no.3, 2015.

[36] T. Parks, and J. McClellan, "Chebyshev approximation for nonrecursive digital filters with linear phase," *IEEE Trans. on Circuit Theory*, vol. 19, No. 2, pp. 189-194, 1972.

[37] J. S. Hong, and M. J. Lancaster, "Design of highly selective microstrip bandpass filters with a single pair of attenuation poles at finite frequencies," *IEEE Trans. on Microwave Theory and Techniques*, vol. 48, No. 7, pp. 1098-1107, 2000.

[38] A. Kachenoura, L. Albera, L. Senhadji, and P. Comon, "ICA: a potential tool for BCI systems," *IEEE Signal Processing Mag.*, vol. 25, no. 1, pp. 57-68, 2008.

[39] L. Ghosh, A. Konar, P. Rakshit and A. K. Nagar, "Hemodynamic analysis for cognitive load assessment and classification in motor learning tasks using type-2 fuzzy sets," *IEEE Trans. on Emerging Topics in Computational Intelligence*, vol. 3, no. 3, pp. 245-260, 2018.

[40] F. Song, Z. Guo and D.Mei, "Feature selection using principal component analysis," *International conference on system science, engineering design and manufacturing informatization*, Vol. 1, pp. 27-30, IEEE, 2010.

[41] Q. Du, H. Yang, and N. H. Younan, "Improved sequential endmember extraction algorithms," *in Proc. IEEE Conf. Hyperspectral Image Signal Process.: Evolution Remote Sensing, Lisbon, Portugal*, Jun. 2011, pp. 1–4.

[42] V. S. Devi and M. N. Murty, "*Pattern Recognition-: An introduction*," Univ. Press, Hydrabad, India, 201.

[43] P. Rakshit *et al*., "Realization of an adaptive memetic algorithm using differential evolution and q-learning: a case study in multirobot path planning," *IEEE Trans. Syst. Man, Cybernetics, Syst*., vol. 43, no. 4, pp. 814–831, Jul. 2013.

[44] S. Das, A. Abraham, and A. Konar, "Automatic clustering using an improved differential evolution algorithm," *IEEE Trans. Syst., Man, Cybern. A, Syst. Hum.*, vol. 38, no. 1, pp. 218–237, Jan. 2008.

[45] D. Wu, C. T. Lin, J. Huang, and Z. Zeng, "On the functional equivalence of TSK fuzzy systems to neural networks, mixture of experts, CART, and stacking ensemble regression," *IEEE Trans. on Fuzzy Systems*, Vol. 28, no. 10, pp.2570-2580, 2019.

[46] G. J. Klir and B. Yuan, *Fuzzy Sets and Fuzzy Logic: Theory and Applications*, Pretice-Hall, 1997.

[47] D.Wu, "A constraint representation theorem for interval type-2 fuzzy sets using convex and normal embedded type-1 fuzzy sets, and its application to centroid computation," in *Proc. World Conf. Soft Comput.*, San Francisco, CA, USA, May 2011

[48] D. Wu and J. M. Mendel, "Enhanced Karnik-Mendel Algorithms," *IEEE Trans. Fuzzy Systems*, vol. 17, no.4, pp. 923-934, Aug. 2009.

[49] M. Laha, A. Konar, P. Rakshit, and A. K. Nagar, "Exploration of Subjective Color Perceptual-Ability by EEG-Induced Type-2 Fuzzy Classifiers," *IEEE Trans. on Cognitive and Developmental Systems*, vol. 12, no. 3, pp. 618-635, 2019.

[50] C. Wagner and H. Hagras, "Toward General Type-2 fuzzy logic system based on z-slice," *IEEE Trans. Fuzzy System*, vol. 18, no. 4, pp. 637-660, 2010.

[51] A. Saha, A. Konar, and A. K. Nagar. "EEG Analysis for Cognitive Failure Detection in Driving Using Type-2 Fuzzy Classifiers," *IEEE Trans. Emerging Topics in Computational Intelligence*, vol. 1, no. 6, pp. 437-453, 2017.

[52] World Medical Association, "World medical association declaration of Helsinki. Ethical principles for medical research involving human subjects," *Bull. World Health Organ.*, vol. 79, no.4, pp.373–374, 2001.

[53] D. Purves, R. Cabeza, S. A. Huettel, K. S. LaBar, M. L. Platt, M. G. Woldorff, and E. M. Brannon, "*Cognitive neuroscience*," Sunderland: Sinauer Associates, Inc, 2008.

[54] W. D. Cooper, "*Electronic instrumentation and measurement techniques*," Prentice Hall, 1978.

[55] A. S. Sánchez *et al*., "Application of an SVM-based regression model to the air quality study at local scale in the Avilés urban area (Spain)," *Mathematical and Computer Modelling*, vol. 54, no.5-6, pp. 1453-1466, 2011.

[56] W. Wang, Z. Xu, W. Lu, and X. Zhang, "Determination of the spread parameter in the Gaussian kernel for classification and regression," *Neurocomputing*, vol. 55, no. 3,4, pp. 643-663, 2003.

[57] J. Sun, D. K. Kalenchuk, D. Xue, and P. Gu, "Design candidate identification using neural network-based fuzzy reasoning," *Robotics and Computer-Integrated Manufacturing*, vol. 16, no. 5, pp. 383-396, 2000.

[58] C. L. Goodale, J. D. Aber and S. V. Ollinger. "Mapping monthly precipitation, temperature, and solar radiation for Ireland with polynomial regression and a digital elevation model," *Climate Research*, vol. 1, pp: 35-49, 1998.

[59] F. Aghaeipoor,and M. M. Javidi, "On the influence of using fuzzy extensions in linguistic fuzzy rule-based regression systems," *Applied Soft Computing*, Vol. 79, pp. 283-299, 2019.

[60] D. Bhattacharya, A. Konar, A., and P. Das, "Secondary factor induced stock index time-series prediction using self-adaptive interval type-2 fuzzy sets," *Neurocomputing*, vol. 171, pp. 551-568, 2016.

[61] D. Basu, S. Bhattacharyya, D. Sardar, A. Konar, D. N. Tibarewala, and A. K. Nagar, "A differential evolution based adaptive neural Type-2 Fuzzy inference system for classification of motor imagery EEG signals," *FUZZ-IEEE*, pp. 1253-1260, 2014.

[62] A. Halder, A. Konar, R. Mandal, A. Chakraborty, P. Bhowmik, N. R. Pal, and A. K. Nagar, "General and interval type-2 fuzzy face-space approach to emotion recognition," *IEEE Trans. Systems, Man, and Cybernetics: Systems*, vol. 43, no. 3, pp. 587-605, 2013.

[63] J. Demsar, "Statistical comparisons of classifiers over multiple data sets," *J. Mach. Learn. Res.*, vol. 7, pp. 1–30, Dec. 2006.

[64] f-NIRs datasets used for the present work on olfactory perception. Available:https://drive.google.com/drive/folders/1aTgj2nDj5FwYtl_ymYfYWCn0XFTSS6Hp?usp=sharing. [Online]. How to read data. Available:https://drive.google.com/file/d/1K9xYi2_hgPFeT6CZ9i5BTSfSViqq7k3t/view?usp=sharing. [Online].

[65] Appendix.Available:https://drive.google.com/file/d/1UEk4LG_1vVqcLWORJOZJ1DN8AAh-X6g9/view?usp=sharing. [Online].

Mousumi Laha received her B.Tech. degree in Electronics and Tele-Communication Engineering from Camellia Institute of Technology in 2011, and her M. Tech. degree in Intelligent Automation and Robotics (IAR) from the department of Electronics and Tele-Communication Engineering, Jadavpur University, Kolkata in 2015. She is currently pursuing her Ph.D. in Cognitive Intelligence in Jadavpur University under the guidance of Prof. Amit Konar and Dr. Pratyusha Rakshit. Her current research interest includes type-2 fuzzy sets, brain-computer interfaces, and biological underpinning of cognition and sensory perception.

Amit Konar (SM' 2010) is currently a Professor in the department of Electronics and Tele-Communication Engineering, Jadavpur University, Kolkata, India. He earned his B.E. degree from Indian Institute of Engineering Science and Technology (fromerly, Bengal Engineering College), Sibpur in 1983, and his M.E., M. Phil. and Ph.D. degrees, all from Jadavpur University in 1985, 1988 and 2004 respectively. Dr. Konar has published 15 books and over 350 research papers in leading international journals and conference proceeding. His current research interest includes Cognitive Neuroscience, Brain-Computer Interfaces, Type-2 Fuzzy Sets, Multi-agent Systems and Scientific Creativity.

Pratyusha Rakshit received the B. Tech. degree in Electronics and Communication Engineering (ECE) from Institute of Engineering and Management, India, and M.E. degree in Control Engineering from Electronics and Telecommunication Engineering (ETCE) Department, Jadavpur University, India in 2010 and 2012 respectively. She was awarded her Ph.D. (Engineering) degree from Jadavpur University, India in 2016. She is currently an Assistant Profesor in ETCE Department, Jadavpur University. She has published 2 books and over 60 papers in leading international journals and conference proceedings. Her principal research interests include computational intelligence, evolutionary algorithms, robotics, bioinformatics, cognitive science and human-computer interaction.

Atulya K. Nagar is a Professor of Mathematical Sciences and is the Pro Vice-Chancellor (Research) at Liverpool Hope University, United Kingdom. He is responsible for developing Sciences and Engineering and has been the Head of the School of Mathematics, Computer Science and Engineering which he established at the University. He received a prestigious Commonwealth Fellowship for pursuing his doctorate (DPhil) in Applied Nonlinear Mathematics, which he earned from the University of York (UK) in 1996. He holds BSc (Hons), MSc, and MPhil (with distinction) in Mathematical Physics from the MDS University of Ajmer, India. Prior to joining Liverpool Hope, he was with the Brunel University, London. He is an internationally respected scholar working at the cutting edge of nonlinear mathematics, theoretical computer science, and systems engineering. He has edited volumes on Intelligent Systems, and Applied Mathematics. He is well published with over 450 publications in prestigious publishing outlets. He has an extensive background and experience of working in Universities in the UK and India. He has been an expert reviewer for the Biotechnology and Biological Sciences Research Council (BBSRC) grants peer-review committees for Bioinformatics Panel; Engineering and Physical Sciences Research Council (EPSRC) for High Performance Computing Panel; and served on the Peer-Review College of the Arts and Humanities Research Council (AHRC) as a scientific expert member. Prof Nagar sits on the JISC Research Strategy group and he is a fellow of the Institute of Mathematics and Its applications (FIMA) and a fellow of the Higher Education Academy (FHEA).